Original Research Article

# Cigarette smoke condensate modulates migration of human gingival epithelial cells and their interactions with *Porphyromonas gingivalis*

K. Imamura[1], E. Kokubu[2], D. Kita[1], K. Ota[1, 3], K. Ishihara[2, 3], A. Saito[1, 3]

[1]Department of Periodontology, Tokyo Dental College, Tokyo, Japan
[2]Department of Microbiology, Tokyo Dental College, Tokyo, Japan
[3]Oral Health Science Center, Tokyo Dental College, Tokyo, Japan

**Corresponding author**
Atsushi Saito, DDS, PhD, Department of Periodontology, Tokyo Dental College
2-9-18-8F Misaki-cho, Chiyoda-ku, Tokyo, 101-0061 Japan
Phone: +81-3-6380-9172 E-mail: atsaito@tdc.ac.jp

Running title: Effects of cigarette smoke on gingival epithelial cells

**Key words:** smoking; epithelial cells; gingiva; cell migration; periodontal diseases; Gram-negative bacteria

**Abstract**

*Background and Objective:* Epithelial cells are recognized as the first line of defense against bacterial infection and environmental harmful stimuli such as cigarette smoke (CS). Although previous studies explored the effects of nicotine on host cells, mechanisms by which CS affects cellular functions remain uncertain. The present study investigated the effects of CS condensate (CSC) on *in vitro* wound closure of gingival epithelial cells and their potential interactions with a major periodontal pathogen, *Porphyromonas gingivalis*.

*Methods:* Human gingival epithelial cells (Ca9-22) were treated with CSC for 24 hours. Cell proliferation was determined using a WST-1 assay. Cell migration was assessed using a wound closure model. The expression of integrins was analyzed by confocal scanning laser microscopy (CSLM) and real-time PCR. Intracellular invasion of *P. gingivalis* was evaluated by an antibiotic protection assay and CSLM.

*Results:* Low concentrations (1-10 μg/ml) of CSC showed no significant effect on cell proliferation. CSC demonstrated dual effects on epithelial wound closure of Ca9-22 cells; high concentrations (i.e., 250 μg/ml) significantly inhibited the wound closure whereas low concentrations (i.e., 10 μg/ml) promoted it ($P < 0.01$). CSC induced distinct changes in cytoskeleton. When CSC-exposed cells were infected with *P. gingivalis* for 2 hours, a significant inhibition of wound closure was observed concurrent with a decrease in integrin α3 expression near the wound area. A significantly increased *P. gingivalis* invasion into Ca9-22 was observed when exposed to low concentration of CSC.

*Conclusion:* Non-cytotoxic levels of CSC exert changes in epithelial cell functions by altering cytoskeleton and integrin expression, which can be further modulated by *P. gingivalis* infection.

## Introduction

Numerous epidemiological studies have established that tobacco smoking is a major risk factor for a number of diseases. Cigarette smoking is a well-established risk factor for periodontal disease and is the strongest of the modifiable factors (1). In patients with periodontitis, smoking is associated with loss of attachment and bone resorption (2, 3).

Smoking also exerts negative effects on the response of periodontal tissue to treatment including regenerative procedures (1). Furthermore, there is evidence that smokers harbor a higher prevalence of periodontal pathogens than non-smokers (4, 5).

Epithelial cells that encompass mucosal surfaces are increasingly recognized as the first line of defense against environmental harmful stimuli such as cigarette smoke (CS) (6). Most cells targeted by CS are oral epithelial and bronchial cells. Cell migration and proliferation are key aspects of many biological processes, including wound healing and tissue regeneration (7). During wound healing process, epithelial cells at wound edges start to migrate and proliferate to cover the denuded area. This cell migration is necessary for reepithelialization (8, 9). In case of periodontitis, migration of infected epithelial cells facing the tooth is increased to form periodontal pockets (10). It has been shown that nicotine, major constituent of the particulate phase of CS, alters wound healing response (1, 11). However, information is limited regarding the bacterial and environmental factors that affect periodontal wound healing.

Gingival epithelial cells also function as a mechanically protective barrier against infection by pathogenic organisms. Smoking may modulate susceptibility of epithelial cells to become colonized by periodontal pathogens (12). CS could impair epithelial innate immune responses to microbial products, allowing overgrowth and invasion (13). *Porphyromonas gingivalis*, a gram-negative anaerobe, is a major colonizer of gingival

tissues and has been etiologically implicated in various forms of periodontitis (14). Cellular invasion by *P. gingivalis* is postulated as a potential virulence factor, affording protection from the host immune responses and contributing to tissue damage (15). In addition, invasion of epithelial cells by *P. gingivalis* was demonstrated to inhibit cellular migration and proliferation (7). It was shown that cotinine, one of the most important metabolites of nicotine, affected the association and invasion of epithelial cells by *P. gingivalis* (16). Collectively, these findings led us to hypothesize that smoking modulates interaction between host cells and periodontal pathogens.

CS is a complex mixture of more than 7,000 different chemical constituents (7), which could act individually or collectively as pathogenic agents for different diseases. Although it is relevant to elucidate the effects of nicotine on host cells, these responses must be analyzed in a physiological context, i.e., in the presence of the multiple mixture of components in CS. One *in vitro* strategy to evaluate the effects of CS on host cells is the use of CS condensate (CSC), which is generated through the controlled combustion of the 1R3F research cigarette (18). It has been suggested that CSC affects the extracellular matrix remodeling (19). Furthermore, CSC may affect key cell functions involved in wound repair (20). These findings emphasize the importance of understanding the effects of CS exposure on host cell functions in relation to the infection by periodontal pathogens.

This paper suggests possible hypotheses for the pathological mechanism of CS in periodontal disease, highlighting its effect on the function of human gingival epithelial cells and their interaction(s) with a prominent periodontal pathogen, *P. gingivalis*.

## Materials and methods

### Cells and culture conditions

An established immortalized human gingival epithelial cell line, Ca9-22 (Health Science Research Resources Bank, Osaka, Japan), was cultured as described previously (21). Briefly, Ca9-22 cells were maintained in minimal essential medium (MEM) supplemented with glutamine (Gibco, Invitrogen, Carlsbad, CA, USA), heat-inactivated 10 % fetal bovine serum (Gibco, Invitrogen), and gentamicin (10 µg/ml) / amphotericin B (0.25 µg/ml) (Cascade Biologics, Portland, OR) at 37 °C in 5 % $CO_2$ in humidified air.

### Bacterial strains

*P. gingivalis* ATCC 33277 was routinely maintained on tryptic soy agar (Difco Laboratories, Detroit, MI) supplemented with 10% defibrinated horse blood, hemin (5 µg/ml) and menadione (0.5 µg/ml) at 37 °C under anaerobic conditions (80% $N_2$, 10% $CO_2$, and 10% $H_2$). For the following assays, *P. gingivalis* was grown in brain heart infusion (BHI) broth (Becton Dickinson, Sparks, MD) supplemented with 0.5 % of yeast extract, hemin and menadione. The bacterial cultures were grown to mid-log phase [range at optical density (OD) at 660 nm of 0.6-1.0] at 37 °C under anaerobic conditions.

### Nicotine and Cigarette Smoke Condensate

Nicotine (N3876; Sigma-Aldrich, St Louis, MO) was stored in dark at -4°C. To evaluate the effects of CS on Ca9-22 cells, we used the commercially available CSC (Murty Pharmaceuticals, Lexington, KY), which was prepared from standard research cigarettes (3R4F; University of Kentucky, KY) (22). The percentage of nicotine in the CSC was documented to be 2.4% by the Clinical Pharmacology Laboratory, San Francisco General Hospital, San Francisco, CA (19). The CSC was diluted into dimethyl sulfoxide (DMSO) and aliquots were kept at -80°C. Stock CSC was thawed and added to cell growth media using serial dilutions to create treatment media of desired concentrations. DMSO was used as the vehicle control.

**Epithelial cell viability after exposure to nicotine or CSC**

Ca9-22 cells were grown in flat-bottom culture plates to 80 to 90% confluence and then stimulated with various concentrations of nicotine or ethanol (control) at 37°C for 24 hours. All nicotine solutions were freshly prepared before each experiment. For CSC exposure, Ca9-22 cells were incubated with CSC in DMSO or plain DMSO (control). Effects were tested over a range of nicotine or CS concentrations.

Cell viability after treatment with nicotine or CSC was determined using the trypan blue dye exclusion test. Ca9-22 cell cultures were grown in 6-well tissue culture plates, exposed or not to the various concentrations of nicotine or CSC. Approximately, 2 $x10^5$ cells were inoculated into each well and incubated at 37°C for 4 days to reach a confluent monolayer in MEM. The epithelial cells were incubated with nicotine or CSC for 24 hours. After this period, the medium was removed from the wells and the cells

were washed three times with phosphate buffered saline (PBS) (pH 7.4, Wako Pure Chemical Industries, Osaka, Japan). The cells were then detached from the wells by incubating with 1 ml trypsin-EDTA (TrypLE$^{TM}$ Select, Gibco) diluted in PBS at 37°C for 2 minutes. These cell suspensions were stained for 3 minutes using trypan blue (Merck Millipore Japan, Tokyo, Japan), in a proportion of 1:100 (v/v). The number of viable cells was assessed by manual counting.

**Effect of CSC on cell morphology and cytoskeleton**

Ca9-22 cells were grown on coverslips in six-well tissue culture plates and were incubated with various concentrations of CSC for 24 hours. The effect of CSC on the morphology of Ca9-22 cells was assessed by phase-contrast microscopy (Eclipse TE:DH, 100 W, Nikon, Tokyo).

In order to further observe the effect of CSC on cellular morphology and cytoskeleton, confocal scanning laser microscopy (CSLM) was performed. CSC-treated cells were fixed in 4% paraformaldehyde in PBS for 10 minutes. After washing three times with PBS, any excess of reactive groups paraformaldehyde were quenched with 50 mM $NH_4Cl$ in PBS for 10 minutes at room temperature. After washing, cells were incubated with Alexa Fluor 633 (green fluorescent dye) conjugated to phalloidin (Molecular Probes, Eugene, OR) for 30 minutes according to the manufacturer's recommendations to visualize the cellular cytoskeleton.

Coverslips mounted in an antifading mounting medium (VECTASHEILD, Vector Laboratories, Burlingame, CA) were examined by CSLM using a LSM5 DUO microscope (Carl Zeiss MicroImaging, Göttingen, Germany) with a 63 x oil immersion

objective. A series of 20-25 Z-stack images was scanned in increments using excitation wavelength of 633 nm. Images were analyzed using ZEN 2008 software (Carl Zeiss).

**Effect of nicotine or CSC on cell proliferation**

Cell proliferation after treatment with nicotine or CSC was determined using the modified MTT assay based on the cleavage of tetrazolium salt WST-1 (Premix WST-1 Cell Proliferation Assay System, Takara Bio, Otsu, Japan) to formazan, which is directly proportional to the number of living cells by cellular mitochondrial dehydrogenase. Various concentrations of nicotine or CSC were added to the subconfluent Ca9-22 cells in 96-well plates. After 24 hours, 10 µl of premixed WST-1 reagent was added to each well and incubated for 1 hour for 37 °C in 5% $CO_2$. The resulting supernatants were then measured for absorbance at 450 nm using a microplate reader (SpectraMax M5e, software; Softmax Pro, Molecular Devices, Sunnyvale, CA).

**Effect of CSC and/ or *P. gingivalis* on epithelial wound closure**

To model the physiological environment of epithelial cells in smokers, confluent Ca9-22 monolayers in 6-well plates were incubated with nicotine or CSC with the concentration range that included the saliva concentrations of nicotine (11, 23). After 24 hours, 3 artificial wounds per well were made using a pipette tip as described by Fang and Svododa (9). The sizes of the wound were nearly constant (approximately 500 µm in width) at the beginning of cell migration. The cells were washed quickly to remove the floating detached cells. The wound area was monitored up to 12 hours using a

microscope (Eclipse TE-DH , Nikon) equipped with a digital micro-camera system (FDX-35, Nikon). The cells were maintained in a tissue culture incubator between image acquisitions. The cells were kept at room temperature for 10-15 minutes for photography. The captured images were tracked by using an image processing program (Image J ver.1.47, National Institutes of Health, Bethesda, MD) (http://rsb.info.nih.gov/ij) that measured the area of the *in vitro* wound. Six consecutive microscopic fields were analyzed and averaged. The wound closure percentage was calculated by dividing the wound area (0-12 hours) by the original area.

To determine the effects of *P. gingivalis* infection, these experiments were essentially carried out as described as above, except that in some cases, *P. gingivalis* was added to nicotine or CSC-exposed Ca9-22 cells. *P. gingivalis* 33277 was cultivated as mentioned before ($OD_{660}$ = 1.0). The bacterial cultures were harvested by centrifugation, washed with PBS, and resuspended in MEM. CSC-treated Ca9-22 monolayers were then infected with *P. gingivalis* [2.0 x $10^7$ cells per well; the multiplicity of infection (MOI= 100)] for 2 hours. After washing the monolayers with PBS, the wound assay was performed.

**Assessment of the integrin expression**

CSLM was also used to assess the expression of integrin in the wound closure assay, according to the method described by Sugisawa et al (24). Briefly, the confluent Ca9-22 monolayers in 6-well plates were incubated with or without CSC for 24 hours. The scraped-wound cell sheets were washed twice with PBS and then cultured at 37°C under an atmosphere of 5% $CO_2$. After 2 hours, the cells were fixed with 4%

paraformaldehyde for 20 minutes at room temperature. After washing with PBS, the cells were incubated with 3% bovine serum albumin (BSA) for 30 minutes at room temperature to prevent nonspecific reactions. After removal of the BSA, the cells were incubated overnight at 4°C, with a rabbit polyclonal antibody to integrin α3 (diluted 1:100 with 1% BSA; Merck KGaA, Darmstadt, Germany). After washing in PBS, the cells were incubated with an appropriate secondary antibody [goat anti-rabbit immunoglobulin G (IgG) (diluted 1:500 with 0.5% BSA) – conjugated with Alexa 546], then with phalloidin conjugated with Alexa 633 (diluted 1:500 with 0.5% BSA) (Molecular Probes) to stain actin, for 1 hour at room temperature. The specimens were examined as described earlier.

**RNA preparation and real-time PCR for integrin**

Total RNAs were extracted using the phenol–chloroform method as follows. Sample was homogenized using 100 µl TRIzol Reagent (Invitrogen, Carlsbad, CA) and each solution was transferred to a 1.5 ml tube containing 100 µl chloroform and was mixed. Each tube was centrifuged at 14,000 rpm at 4 °C for 20 minutes, after which each supernatant was placed in a 1.5 ml tube containing 250 µl 100% isopropanol at -80 °C for 1 hour. After centrifugation at 14,000 rpm at 4 °C for 20 minutes, the supernatant was discarded and the remaining total RNA pellet was washed with 70% cold ethanol and then dissolved in 50 µl RNase-free (DEPC-treated) water. The purity of total RNAs was assessed by Nano-drop ND-1000 spectrometer (Thermo Fisher Scientific, Wilmington, DE). One microgram of total RNA was reverse transcribed to cDNA using a commercial kit (ReverTra Ace®, Toyobo, Osaka), according to manufacturers'

instruction. RT-PCR products were analyzed using quantitative real-time RT-PCR in TaqMan Gene Expression Assays (Applied Biosystems, Foster City, CA) for the target genes integrin α3 (Hs01076873_m1; Applied Biosystems) and integrin β4 (Hs00236216_m1). β-actin (Human ACBT: 4333762; Applied Biosystems) was used as endogenous control. PCR was performed using the 7500 Fast Real-Time PCR System (Applied Biosystems). Assays were performed in 20 µl single-plex reactions containing TaqMan Fast Universal PCR MasterMix, TaqMan Gene Expression Assays, RNase-free water and 1 µg cDNA following the protocol of manufacture (Applied Biosystems). The CT values of target genes were normalized with β-actin.

**Assessment of bacterial invasion**

*P. gingivalis* invasion of gingival epithelial cells was assessed by a standard antibiotic protection assay as described previously (21) with slight modifications. Briefly, subconfluent Ca9-22 cells in 12-well flat-bottom culture plates were washed twice with PBS and resuspended in MEM without antibiotics. Following addition of various concentrations of CSC, the cells were incubated for 24 hours at 37 °C in 5 % $CO_2$ . Prior to bacterial infection, the wells were washed three times with PBS. The *P. gingivalis* suspensions were then added to the monolayers (MOI= 100) and incubated for 2 hours. In some experiments, the bacterial suspensions were added without washing the wells, thus allowing the bacteria to be exposed to nicotine or CSC. After incubation, unattached bacteria were removed following washing of the monolayers 3 times with PBS. External adherent cells were then killed by incubating the infected monolayers with MEM containing 200 µg/ml of metronidazole and 300 µg/ml of gentamicin for 1

hour. After exposure to antibiotic, monolayers were washed twice with PBS, and lysed in 1 ml of sterile distilled water per well. Cells were incubated for 30 minutes, during which they were disrupted by repeated pipetting. Lysates were serially diluted and plated on blood agar plates supplemented with hemin and menadione, and incubated anaerobically at 37 °C for 10 days. Colony-forming units of invasive organisms were then enumerated. Invasion efficiency was expressed as the percentage of the initial inoculum recovered after antibiotic treatment and Ca9-22 lysis. The monolayers were checked microscopically prior to each invasion experiment. No significant differences between control monolayers and CSC inoculated monolayers could be observed.

**Visualization of *P. gingivalis* invasion**

Following treatment of Ca9-22 cells with CSC, *P. gingivalis* invasion was assessed. The protocol for visualization of bacterial internalization into gingival epithelial cells by CSLM was reported previously (25). In brief, Ca9-22 cells were grown on coverslips in six-well tissue culture plates and infected with *P. gingivalis* suspensions (MOI=100) for 2 hours. After fixation and washing, cells were incubated with a rabbit polyclonal anti-*P. gingivalis* serum diluted 1:500 in PBS-0.5% BSA for 60 minutes. Following incubation, coverslips were washed three times with PBS and incubated with Alexa Fluor 488 (green fluorescent dye)-conjugated goat anti-rabbit IgG (Molecular Probes) diluted 1:500 for 30 minutes to visualize attached, extracellular bacteria. Internalized bacteria were stained by first permeabilizing Ca9-22 cells by dipping coverslips in 0.4% Triton X-100 solution for 5 minutes, then staining with the rabbit anti-*P. gingivalis* serum followed by Alexa Fluor 568 (red fluorescent dye)-coupled goat anti-rabbit IgG

(Molecular Probes) diluted 1:500 as described above. Actin filaments were stained with Alexa Fluor 633 conjugated to phalloidin for 30 minutes according to the manufacturer's recommendations to visualize the cellular cytoskeleton and confirm internalization. Mounted coverslips were examined by CSLM and images were analyzed as described earlier.

**Statistical analysis**

All experiments were performed in duplicate or triplicate for each condition and repeated at least three times. Statistical comparisons were performed by Student t test or analysis of variance (ANOVA) with Tukey post test, using a software package (InStat 3.10, GraphPad Software, La Jolla, CA). A *P*-value less than 0.05 was considered significant.

## Results

### Cell viability and proliferation after treatment

With concentrations in the range of 1 to 100 µg/ml, nicotine showed no significant effect on the viability of Ca9-22 cells in 24-hour incubation, as assessed by the trypan blue exclusion (data not shown). Survival was greater than 85% at these concentrations. When nicotine concentration was increased to 200 µg/ml, a significant reduction in viability was observed; it was reduced to less than 10%. Although CSC exposure in the range of 1 to 100 µg/ml exerted no effect on the cell viability, CSC at 300 µg/ml (estimated nicotine conc. 7.2 µg/ml) showed a significant cytotoxic effect: the viability was reduced to 30% of the untreated control (data not shown).

The effect of nicotine or CSC on cell proliferation was studied using WST-1 cell proliferation assay in subconfluent cultures of Ca9-22 cells. The results of the WST-1 assay followed a general trend of trypan blue exclusion: nicotine in the range of 1 to 50 µg/ml showed no significant effect on the cell proliferation (Fig.1A ). Lower concentrations of CSC showed no significant effect on cell proliferation, whereas higher concentrations (50 to 200 µg/ml) exerted a statistically significant but slight increase in cell proliferation (Fig.1B ). When the CSC concentration was increased to 300 µg/ml, cell proliferation was almost completely inhibited (data not shown).

### Morphological and cytoskeletal changes induced by CSC

The effect of CSC on the morphology of Ca9-22 cells was assessed by phase-contrast

microscopy. Untreated cells (control) showed regular shape (Fig. 2A). No significant vacuolization of the cells was observed by the addition of CSC with the concentration range of 1.0 to 250 µg/ml. CSC at 10 µg/ml induced a distinct change in morphology of Ca9-22 cells in 24 hours. The lamellipodia-like cell protrusions became longer and increased in number. When the concentration was increased to 250 µg/ml, the cells became roundish and lamellipodia-like cell protrusions were decreased.

CSLM observation showed actin rearrangement in cells treated with 10 µg/ml CSC (Fig. 2B). When the CSC concentration was increased to 250 µg/ml, distinct aberrations in the cellular morphology and arrangement of actin cytoskeleton were observed.

**_In vitro_ wound closure in response to various concentrations of CSC**

In the wound assay, nicotine at 0.1 µg/ml promoted wound closure of Ca9-22 cells in 12 hours (Fig. 3A and Fig. 3B), whereas high concentrations (i.e., 50 µg/ml) inhibited it. Within the concentration range that showed no significant cytotoxic effects, CSC demonstrated dual effects on wound closure: low concentrations (0.1-10 µg/ml) showed a dose-dependent increase in wound closure whereas high concentrations showed a tendency for inhibition (Fig.3A and Fig. 3C). The maximal inhibition occurred at concentration of 250 µg/ml CSC (nicotine conc. 6.0 µg/ml).

**Effect of _P. gingivalis_ challenge on wound closure**

When Ca9-22 cells pre-exposed to CSC were infected with *P. gingivalis* ATCC 33277 for 2 hours, inhibition of wound closure was observed over the concentration range of

CSC examined (Table 1). At the concentration range of 1-50 µg/ml, the inhibition induced by *P. gingivalis* infection was statistically significant; the rate of wound closure was reduced to approximately 60-70% of the uninfected group. The trend for wound closure enhancement previously demonstrated at lower CSC concentrations was not observed in the presence of *P. gingivalis*.

**Differential expression of integrin α3 in response to the CSC and/or *P. gingivalis***

Positive reactivity for integrin α3 was observed as red fluorescence and was detected in the control cells without CSC (Fig. 4). In cells around the wound area, immunoreactivity for integrin α3 was most strongly observed and extended in the proximal cytoplasm to the scraped area. Exposure of Ca9-22 cells to ~10 µg/ml CSC for 24 hours resulted in a general increase in the integrin expression (Fig. 4A). When the concentration of CSC was increased to 250 µg/ml, the immunoreactivity for integrin was reduced. In the presence of *P. gingivalis*, no increase in the integrin expression was observed in Ca9-22 cells exposed to 10 µg/ml CSC (Fig. 4B).

To verify the integrin α3 expression at transcription level, mRNA expression in Ca9-22 was quantified using real time-PCR, and compared to that of integrin β4. Treatment with 10 µg/ml CSC yielded a significant increase in integrin α3 mRNA expression (Fig. 4C), collaborating the CSLM findings. The presence of *P. gingivalis* induced a reduction in the mRNA expression at this CSC concentration. In the cells exposed to high concentration of CSC, the expression of integrin α3 mRNA showed some increase (to near control level) in the presence of *P. gingivalis*.

No significant difference in integrin β4 expression was noted when Ca9-22 cells were treated with CSC with or without the presence of *P. gingivalis* (Fig. 4D).

### *P. gingivalis* invasion into CSC-treated cells

In order to explore the mechanism(s) of the modulation of wound closure by *P. gingivalis*, we next assessed the role of bacterial invasion. Intracellular invasion of CSC-treated Ca9-22 cells by *P. gingivalis* 33277 was confirmed by CSLM (Fig. 5A, B) and quantified by the antibiotic protection assay (Fig. 5C). When only the host cells were exposed to CSC, no significant differences in bacterial invasion was observed with different CSC concentrations (data not shown). There was, however, more than a 70% increased invasion in the 1 µg/ml CSC group compared to control, when the host cells and *P. gingivalis* were both exposed to the substance (Fig. 5A, B, C). Over a 2-hour period, no significant differences in bacterial viability could be detected between control media and CSC-treated media (data not shown).

## Discussion

Environmental stimuli such as CS have profound impacts on human cells, with implications for a wide variety of disease processes (26). Previous studies have explored the role of nicotine on the altered wound healing response described in smokers. However, only recent studies have analyzed the role of the whole mixture of components present in CS that may affect cell responses involved in periodontal tissue repair (19, 20, 27, 28). In the present study, using a gingival epithelial cell line as a model, we evaluated *in vitro* the effects of CSC on host cell viability, proliferation, migration and potential interaction with a major periodontal pathogen, *P. gingivalis*. This study provides experimental evidence for the first time that non-lethal levels of CSC exert concentration-dependent biphasic effects on migration of gingival epithelial cells, which can be modulated by *P. gingivalis* infection.

It is of particular interest to note that at lower concentrations, nicotine promoted the wound closure of Ca9-22 cells. In our assays, we used nicotine with the concentration range relative to what was reported in saliva of smokers (11, 23). The effect of physiologically relevant levels of nicotine on host cell migration is contradictory, with stimulation (29) and inhibition (9) being reported. The difference may be because of different nicotine concentrations, exposure times or source of nicotine, given the fact that concentration of nicotine in human serum or saliva varies depending on the levels of smoking. It is possible that other factors such as presence of serum or growth factors, cell types, direction of migration, and/or assay conditions may also affect the results.

Similarly, our data demonstrated that, at lower concentrations, CSC promoted the epithelial wound closure, while it had no marked effect on cell proliferation. This

observation is consistent with prior studies demonstrating an increased wound closure by human gingival fibroblast (20) and bronchial epithelial cell lines (30). At CSC concentration of 10 μg/ml, phase-contrast microscopic examinations revealed the formation of long lamellipodia-like cell protrusions. A similar cell behavior is considered to be involved in the morphogenesis of tissues during periodontal disease and regeneration processes (31). Actin filaments play central roles in the shaping of cells, the maintenance of cell integrity, and stability of cytoskeletal interaction, as well as cell substrate adhesion (32). In our experiment, changes in actin arrangement were observed by CSC incubation. These changes in cell morphology and cytoskeleton induced by CSC may be responsible for the modulation of wound closure.

On the contrary, with higher concentrations of CSC (≥ 100 μg/ml), a dose-dependent decrease in wound closure of Ca9-22 cells was observed, and at 250 μg/ml (estimated nicotine concentration 6 μg/ml), a significant reduction, approximately 60%, was noted compared to the control value. Considering that no significant reduction was noted with the comparable concentrations (1-10 μg/ml) of nicotine, our findings suggest that constituents of CS other than nicotine may play a significant role in this inhibition of the wound closure.

Epithelial wound closure is mediated by both cell migration and proliferation (30). Loss of host cell cycle control by increased proliferation may affect periodontal tissue repair and initiate bacterial penetration into periodontal tissues (31). Thus, it seemed possible that modulation of the wound closure observed in CSC-treated Ca9-22 cells was due to the changes in cell proliferation. In the present study, however, exposure with lower concentrations of CSC (< 10 μg/ml) exerted no significant effect on the proliferation of the Ca9-22 cells, as assessed by WST-1 cell proliferation assay.

We next investigated the relationship of wound closure and the localization of adhesive factors under the influence of CSC. Integrins serve as a major family of transmembrane proteins that act as extracellular receptors. Integrins play critical roles in cell adhesion, migration, signal transduction and gene expression (33). In a wound closure model using rat oral epithelial cells, integrin α3 was shown to be expressed at the side towards the extension of cells, suggesting its role in cell migration (24). We demonstrated that 24-hour exposure of Ca9-22 cells to ~10 μg/ml CSC resulted in a general increase in integrin expression. In cells near the wound area, immunoreactivity for integrin α3 was strongly expressed in the peripheral cytoplasm. These findings are consistent with a previous study demonstrating that CS increased the expression of integrins in host cells (34). Integrin modulation may be at least one of the mechanisms by which CSC affects wound closure of the gingival epithelial cells.

During bacterial wound infection epithelial migration may be increased or decreased, depending on the type and amount of bacteria (10). Our study showed that infection with live *P. gingivalis* cells abrogated the wound closure by Ca9-22 cells pre-exposed to CSC. In the presence of *P. gingivalis*, the integrin expression was reduced in the CSC-treated cells. Previous research suggested that measuring protein expression may give biased results when working with viable *P. gingivalis*, due to its proteolytic activity (35). Therefore, we assessed mRNA expression for integrin α3. The results from the real-time PCR were consistent with the CSLM findings: in the presence of *P. gingivalis*, the expression of integrin α3 appeared to show some decrease in the Ca9-22 cells treated with low concentration of CSC. Heat shock protein 60 from *Aggregatibacter actinomycetemcomitans* was shown to significantly affect epithelial cell migration through modulation of integrin α6 expression (36). Unexpectedly, in the cells exposed to

high concentration of CSC, the expression of integrin α3 mRNA showed some increase in the presence of *P. gingivalis*. At this time, we cannot provide an explanation for this, but this phenomenon may not be so relevant given the fact that the increase was at the level of the unexposed (to CSC) cells. These results suggest that periodontopathic bacterial factors may influence tissue repair through modification of integrins.

In order to better understand the effect of CS and/or *P. gingivalis* infection on epithelial wound closure, we set out to investigate *P. gingivalis* invasion into gingival epithelial cells stimulated by CSC. Components in the CS are considered to be capable of altering properties of epithelial cell surfaces. The presence of CS has been shown to increase both biofilm formation and host cell adherence by *Staphylococcus aureus* (26). In the present study, with 1 μg/ml of CSC, a significantly increased *P. gingivalis* invasion was observed only when both the host cells and bacteria were exposed to CSC. In order to gain access into non-phagocytes, bacteria need to modify some host cell functions. It was reported that nicotine enhances meningitic *Escherichia coli* invasion of human endothelial cells through modulation of cytoskeleton (37). *P. gingivalis* has been shown to utilize actin rearrangement to invade into gingival epithelial cells (15). In the present study, we observed the actin rearrangement of Ca9-22 cells in response to low concentration of CSC, and this may partially explain the increased invasion of *P. gingivalis*.

It was reported that invasion of epithelial cells by *P. gingivalis* inhibited cellular migration and proliferation (7). *P. gingivalis* fimbriae has been shown to efficiently invade epithelial cells and degrade focal adhesion components with Arg-gingipain, which causes cellular impairment during wound healing (38). In the present study, the decrease in wound closure of control cells (not exposed to CSC) by *P. gingivalis*

infection was not statistically significant (Table 1). This can be attributed to the difference in assay condition, namely types of *P. gingivalis* fimbriae and the duration of *P. gingivalis* infection.

The possible mechanisms for the increased intracellular invasion by *P. gingivalis* should be interpreted in terms of the effects of CSC on host cells as well as on pathogens. In this study, CSC in the culture media after the 24-hour incubation exerted no significant effects on bacterial viability during the 2-hour infection period. Mechanistically, it is known that smoke exposure alters the activity of multiple *P. gingivalis* genes and the expression levels of several membrane proteins. Studies show augmentation of dental plaque-associated biofilms owing to increased production of *P. gingivalis* fimbrial protein in the presence of CS (39) and altered expression of outer membrane protein leading to suppression of the proinflammatory cytokine response mediated by *P. gingivalis* (40, 41).The exact effects of CS on the physiology and pathogenic potential of *P. gingivalis* remains to be clarified.

CSC exposure induced production of lamellipodia-like structures in the host cells. Bacterial binding to the tips of the epithelial lamellipodia may disrupt the functions of localizing and harnessing actin polymerization for cell motility (31). In the pathogenesis of periodontal disease, bacterial binding to the lamellipodia of gingival epithelial cells may disrupt tissue repair by hindering the cell-cell and cell-matrix contacts. The lamellipodia of migrating epithelial cells have been suggested to become targets for *Prevotalla intermedia* binding (31). Bacteria usually target cellular adhesion molecules, such as integrin, fibronectin, and laminin, to adhere to and invade host cells (24), and *P. gingivalis* adhesion to epithelial cells has been considered to be facilitated by cellular α5β1 integrin (43). Given these findings, it can be speculated that *P. gingivalis* targeted

the cellular adhesion molecules expressed in the CSC-treated Ca9-22 cells allowing their adhesion to and invasion of the host cells.

In relation to the observed dual effects of CSC on *in vitro* wound closure of gingival epithelial cells, it can be interpreted that inhibition may mean reduced cell migration that leads to compromised healing of periodontal tissue. Although increased epithelial wound closure by CSC may appear to be a beneficial effect, such phenomenon in the bronchial epithelial cells has been implicated in the development of lung cancer (30). Our findings also illustrate the delicate equilibrium between epithelial cells and periodontal pathogens that can be disrupted by the exposure to insults such as CS.

Effect of CS on human being is determined by many factors such as type of cigarette, manner and history of smoking (44). In this study, we used a gingival epithelial cell line as surrogate target cells for effects that may occur in the true target tissues *in vivo*. It is likely that the *in vivo* exposure of cells to toxins in inhaled smoke will differ, due to the different concentrations of toxins and to the modulatory effects of proteins and other factors present in the cellular milieu. The translation of 'liquid smoke' to *in vivo* situations is complicated by the different compositions of liquid extract and gaseous smoke, and by an inability to predict the appropriate concentrations and durations of exposure that relate to actual smoking (45).

Despite these limitations, however, *in vitro* experiments with CSC have a history of providing useful information (19, 27, 46). CSC is composed of major toxicants such as nicotine, phenol, anthracyclic hydrocarbons, nitrosamines, heavy metals and chemical carcinogens, such as 4-(methylnitrosamino)-1-(3-pyridyl)-1-butanone (27). The results from the present study also suggest that bioactive constituents of CS other than nicotine may affect the interactions between periodontal pathogens and host cells.

In conclusion, our findings indicate that CSC exerts a concentration-dependent biphasic impact on epithelial cell migration, which can be modulated by the interaction with *P. gingivalis*. This finding provides evidence for a potential mechanism by which CS components induce predisposition to periodontal infection and inhibition of periodontal tissue healing. A better understanding of the mechanisms by which CS affects cell functions in relation to bacterial infection may lead to improved interventions for the prevention and treatment of smoking- associated oral diseases including periodontitis.

**Acknowledgements**

This work was supported in part by Grants-in-Aid for Scientific Research (C) 22592317 and (C) 25463228 (to AS) from Japan Society for Promotion of Science.

The authors report no conflicts of interest related to this study.

## References


1. Johnson GK, Guthmiller JM. The impact of cigarette smoking on periodontal disease and treatment. *Periodontol 2000* 2007;**44:**178-194.
2. Grossi SG, Zambon JJ, Ho AW, et al. Assessment of risk for periodontal disease (I). Risk indicators for attachment loss. *J Periodontol* 1994;**65:**260-267.
3. Tomar SL, Asma S. Smoking-attributible periodontitis in the United States. Findings from NHANES III. National Health and Nutritional Examination Survey. *J Periodontol* 2000;**71:**743-751.
4. Zambon JJ, Grossi SG, Matchei EE, Ho AW, Dunford R, Genco RJ. Cigarette smoking increases the risk for subgingival infection with periodontal pathogens. *J Periodontol* 1996;**67:**1050-1054.
5. van Winkelhoff AJ, Bosch-Tijhof CJ, Winkel EG, van der Reijden WA. Smoking affects the subgingival microflora in periodontitis. *J Periodontol* 2001;**72:**666-671.
6. Preciado D, Lin J, Wuertz B, Rose M. Cigarette smoke activates NFκB and induces Muc5b expression in mouse middle ear cells. *Laryngoscope* 2008;**118:**464-471.
7. Nakagawa I, Inaba H, Yamamura T, et al. Invasion of epithelial cells and proteolysis of cellular focal adhesion components by distinct types of *Porphyromonas gingivalis* fimbriae. *Infect Immun* 2006;**74:**3773-3782.
8. O'Toole EA. Extracellular matrix and keratinocyte migration. *Clin Exp Dermatol* 2001;**26:**525-530.
9. Fang Y, Svoboda KK. Nicotine inhibits human gingival fibroblast migration via modulation of Rac signalling pathways. *J Clin Periodontol* 2005;**32:**1200-1207.
10. Häkkinen L, Uitto V-J, Larjava H. Cell biology of gingival wound healing.

*Periodontol 2000* 2000;**24:**127-152.

11. Giannopoulou C, Roehrich N, Mombelli A. Effect of nicotine-treated epithelial cells on the proliferation and collagen production of gingival fibroblasts. *J Clin Periodontol* 2001;**28:**769-775.
12. Teughels W, Van Eldere J, van Steenberghe D, Cassiman JJ, Fives-Taylor P, Quirynen M. Influence of nicotine and cotinine on epithelial colonization by periodontopathogens. *J Periodontol* 2005;**76:**1315-1322.
13. Kulkarni R, Rampersaud R, Aguilar JL, Randis TM, Kreindler JL, Ratner AJ. Cigarette smoke inhibits airway epithelial cell innate immune responses to bacteria. *Infect Immun* 2010;**78:**2146-2152.
14. Socransky SS, Haffajee AD. The bacterial etiology of destructive periodontal disease: current concepts. *J Periodontol* 1992;**63:**322-331.
15. Lamont RJ, Chan A, Belton CM, Izutsu KT, Vasel D, Weinberg A. *Porphyromonas gingivalis* invasion of gingival epithelial cells. *Infect Immun* 1995;**63:**3878-3885.
16. Cogo K, Calvi BM, Mariano FS, Franco GCN, Gonçalves RB, Groppo FC. The effects of nicotine and cotinine on *Porphyromonas gingivalis* colonisation of epithelial cells. *Arch Oral Biol* 2009;**54:**1061-1067.
17. Rodgman A, Perfetti TA eds. *The chemical components of tobacco and tobacco smoke.* Boca Raton: CRC Press, 2008: 1840.
18. College of Agriculture c/o Kentucky Tobacco Research & Development Center. *Reference cigarette program*. Lexington:University of Kentucky, 1974.
19. Zhang W, Song F, Windsor LJ. Effects of tobacco and *P. gingivalis* on gingival fibroblasts. *J Dent Res* 2010;**89:**527-531.
20. Silva D, Cáceres M, Arancibia R, Martínez C, Martínez J, Smith PC. Effects of

cigarette smoke and nicotine on cell viability, migration and myofibroblastic differentiation. *J Periodont Res* 2012;**47:**599-607.

21. Saito A, Inagaki S, Kimizuka R, et al. *Fusobacterium nucleatum* enhances invasion of human gingival epithelial and aortic endothelial cells by *Porphyromonas gingivalis*. *FEMS Immunol Med Microbiol* 2008;**54:**349-355.
22. Diana JN and Vaught A. *Research cigarettes.* Lexington: The University of Kentucky Printing Services, 1990.
23. Robson N, Bond AJ, Wolff K. Salivary nicotine and cotinine concentrations in unstimulated and stimulated saliva. *Afr J Pharm Pharmacol* 2010;**4:**61-65.
24. Sugisawa M, Masaoka T, Enokiya Y, et al. Expression and function of laminin and integrins on adhesion/migration of primary culture cells derived from rat oral epithelium. *J Periodont Res* 2010;**45:**284-291.
25. Saito A, Inagaki S, Ishihara K. Differential ability of periodontopathic bacteria to modulate invasion of human gingival epithelial cells by *Porphyromonas gingivalis*. *Microb Pathog* 2009;**47:**329-333.
26. Kulkarni R, Antala S, Wang A, et al. Cigarette smoke increases *Staphylococcus aureus* biofilm formation via oxidative stress. *Infect Immun* 2012;**80:**3804-3811.
27. Gonzalez R, Arancibia R, Cáceres M, Martínez J, Smith PC. Cigarette smoke condensate stimulates urokinase production through the generation of reactive oxygen species and activation of the mitogen activated protein kinase pathways in human gingival fibroblasts. *J Periodont Res* 2009;**44:**386-394.
28. Semlali A., Chakir J, Goulet JP, Chmielewski W, Rouabhia M. Whole cigarette smoke promotes human gingival epithelial cell apoptosis and inhibits cell repair processes. *J Periodont Res* 2011;**46:**533-541.

29. Grando SA, Horton RM, Pereira EF, et al. A nicotinic acetylcholine receptor regulating cell adhesion and motility is expressed in human keratinocytes. *J Investig Dermatol* 1995;**105:**774-781

30. Luppi F, Aarbiou J, van Wetering S, et al. Effects of cigarette smoke condensate on proliferation and wound closure of bronchial epithelial cells in vitro: role of glutathione. *Respir Res* 2005;**6:**140

31. Gursoy UK, Könönen E, Uitto VJ. *Prevotella intermedia* ATCC 25611 targets host cell lamellipodia in epithelial cell adhesion and invasion. *Oral Microbiol Immunol* 2009;**24:**304-309.

32. Colombo G, Dalle-Donne I, Orioli M, et al. Oxidative damage in human gingival fibroblasts exposed to cigarette smoke. *Free Radic Biol Med* 2012;**52:**1584-1596.

33. Larjava H, Haapasalmi K, Salo T, Wiebe C, Uitto VJ. Keratinocyte integrins in wound healing and chronic inflammation of the human periodontium. *Oral Dis* 1996;**2:**77-86.

34. Bulmanski Z, Brady M, Stoute D, Lallier TE. Cigarette smoke extract induces select matrix metalloproteinases and integrin expression in periodontal ligament fibroblasts. *J Periodontol* 2012;**83:**787-796.

35. Calkins CC, Platt K, Potempa J, Travis J. Inactivation of tumor necrosis factor alpha by proteinases (gingipains) from the periodontal pathogen, *Porphyromonas gingivalis*. Implications of immune evasion. *J Biol Chem* 1998;**273:**6611-6614.

36. Zhang L, Koivisto L, Heino J, Uitto VJ. Bacterial heat shock protein 60 may increase epithelial cell migration through activation of MAP kinases and inhibition of a6b4 integrin expression. *Biochem Biophys Res Comm* 2004;**319:**1088-1095.

37. ChenY, Chen SH, Jong A, Zhou ZY, Li W, Suzuki K, Huang SH, Enhanced

*Escherichia coli* invasion of human brain microvascular endothelial cells is associated with alterations in cytoskeleton induced by nicotine. *Cellular Microbiol* 2002;**4:**503-514.

38. Kato T, Kawai S, Nakano K, et al. Virulence of *Porphyromonas gingivalis* is altered by substitution of fimbria gene with different genotype. *Cellular Microbiol* 2007;**9:**753-765.
39. Bagaitkar J, Daep CA, Patel CK, Renaud DE, Demuth DR, Scott DA. Tobacco smoke augments *Porphyromonas gingivalis - Streptococcus gordonii* biofilm formation. *PLoS ONE*. 2011;**6:**e27386.
40. Bagaitkar J, Williams LR, Renaud DE, et al. Tobacco-induced alterations to *Porphyromonas gingivalis*-host interactions. *Environ Microbiol* 2009;**11:**1242-1253.
41. Bondy-Carey JL, Galicia J, Bagaitkar J, et al. Neutrophils alter epithelial response to *Porphyromonas gingivalis* in a gingival crevice model. *Mol Oral Microbiol* 2013; **28:**102-113.
42. Hauck CR, Agerer F, Muenzner P, Schmitter T. Cellular adhesion molecules as targets for bacterial infection. *Eur J Cell Biol* 2006;**85:**235-242.
43. Tsuda K, Furuta N, Inaba H, et al. Functional analysis of α5β1 integrin and lipid rafts in invasion of epithelial cells by *Porphyromonas gingivalis* using fluorescent beads coated with bacterial membrane vesicles. *Cell Struct Funct* 2008;**33:**123-132.
44. Liu X, Togo S, Al-Mugotir M, et al. NF-kappa B mediates the survival of human bronchial epithelial cells exposed to cigarette smoke extract. *Respir Res* 2008;**9:**66.
45. Minematsu N, Blumental-Perry A, Shapiro SD. Cigarette smoke inhibits engulfment of apoptotic cells by macrophages through inhibition of actin rearrangement. *Am J Respir Cell Mol Biol* 2011;**44:**474-482.

46. Schembri F, Sridhar S, Perdomo C, et al. MicroRNAs as modulators of smoking-induced gene expression changes in human airway epithelium. *Proc Natl Acad Sci USA* 2009;**106:**2319-2324.

**Figure legends**

*Fig. 1.*

Effect of nicotine (A) or CSC (B) on proliferation of gingival epithelial cells. Various concentrations of nicotine or CSC were added to the Ca9-22 cells grown in 96-well plates, and compared to untreated control. After 24 hours, cell proliferation was assessed by WST-1 assay. Data are shown as means ± standard deviations (n=12) from a typical experiment. *$P < 0.05$, **$P < 0.01$, compared to the untreated control, ANOVA with Tukey post test.

*Fig. 2.*

Effect of CSC on the morphology and cytoskeleton of Ca9-22 cells. Ca9-22 cells were grown on coverslips in six-well plates and were incubated with various concentrations of CSC for 24 hours.

(A) Representative phase-contrast images. (B) Representative CSLM images of the cytoskeletal changes (green fluorescent; actin).

*Fig. 3.*

Representative microphotographs of the wound closure exposed to nicotine or CSC (A). Ca9-22 monolayers cultured to confluence, and various concentrations of nicotine or CSC were added and further incubated for 24 hours. Then multiple artificial wounds were made, and the wound area was monitored up to 12 hours.

The rate of wound closure of Ca9-22 cells following treatment with nicotine (B) or CSC (C). This was obtained using the following formula: (initial wound area) – (wound area after an identified culture period) / (initial wound area) x 100. Values are shown as means ± standard deviations (n= 18) of triplicate independent determinations from a typical experiment. **$P < 0.01$, compared to the untreated control, ANOVA with Tukey post test.

*Fig. 4.*

Representative CSLM images of the cellular distribution of integrin α3 in the scraped-wound Ca9-22 cells. Confluent Ca9-22 monolayers in 6-well plates were incubated with various concentrations of CSC for 24 hours. The cells were incubated further 2 hours in the absence (A) or in the presence (B) of *P. gingivalis* ATCC 33277. Two hours after the artificial wounds were made, the cells were labeled for integrin α3 (red) and actin (green). Asterisks indicate wound areas. Bar:20 μm.

The quantitative analysis of the expression of integrin α3 (C) and β4 (D) mRNA in Ca9-22 cells after the 24-hour incubation with CSC. Relative expression values are shown as mean ± standard deviations (n= 12) of triplicate independent determinations from a typical experiment.

$^{\dagger}P < 0.05$, compared to the untreated control (DMSO only), ANOVA with Tukey post test.

*Fig. 5.*

Invasion of untreated (DMSO only) (A) or CSC (1 μg/ml) -treated (B) Ca9-22 by *P. gingvalis* visualized by CSLM. *P. gingivalis* 33277 invading Ca9-22 cells were stained red, while extracellular bacteria were detected as green-yellow. The host cell cytoskeletons stained with phalloidin appear blue. An increase in the number of intracellular bacteria is observed in CSC-treated Ca9-22 cells (B). This is the representative of the most common pattern of *P. gingivalis* invasion. Bar: 20 μm.

Relative invasion of *P. gingivalis* 33277 into Ca9-22 cells treated with CSC (bacteria pre-exposed to CSC) (C). Invasion efficiency was assessed by an antibiotic protection assay, and data are reported as mean ± standard deviations (n= 36) relative to the untreated (DMSO only) control (invasion efficiency of the control was approximately 0.17%). Results represent three to six independent experiments.

$*P < 0.05$, $**P < 0.01$, compared to the untreated control (DMSO only), ANOVA with Tukey post test.

Table 1.
Effect of *P. gingivalis* infection on epithelial wound closure of CSC-treated Ca9-22 cells.

| CSC (μg/ml) | Wound closure (%) | | Difference |
|---|---|---|---|
| | *P. gingivalis* 33277 | | |
| | - | + | |
| control (DMSO) | 68.9 ± 19.4 | 64.0 ± 16.7 | Ns |
| 0.1 | 81.7 ± 20.5 | 62.1 ± 18.9 | Ns |
| 1 | 87.2 ± 19.3 | 64.4 ± 18.0 | *$P < 0.05$ |
| 10 | 98.6 ± 3.1 | 61.4 ± 20.5 | *$P < 0.001$ |
| 50 | 84.8 ± 21.2 | 58.4 ± 20.7 | *$P < 0.01$ |
| 150 | 58.0 ± 24.0 | 52.7 ± 20.2 | Ns |
| 250 | 25.3 ±13.3 | 23.7 ± 17.5 | Ns |

Values given as mean ± standard deviations of triplicate independent determinations from a typical experiment (n=18).
*Statistically significantly different from uninfected group by Student t test.
ns: not significant

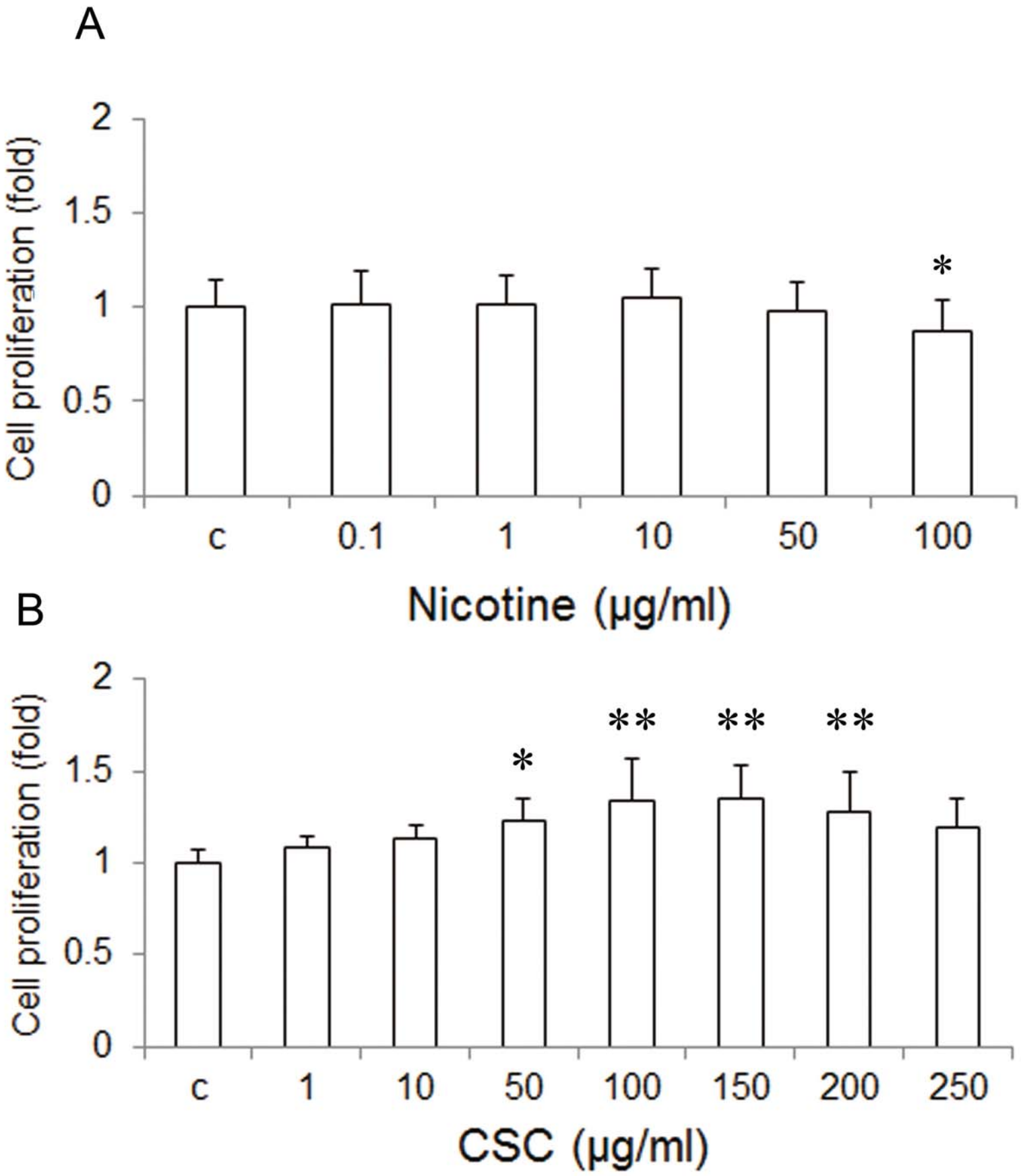
A
Cell proliferation (fold)
2
1.5
1
0.5
0
*
c
0.1
1
10
50
100
Nicotine (μg/ml)
B
Cell proliferation (fold)
2
1.5
1
0.5
0
*
**
**
**
c
1
10
50
100
150
200
250
CSC (μg/ml)

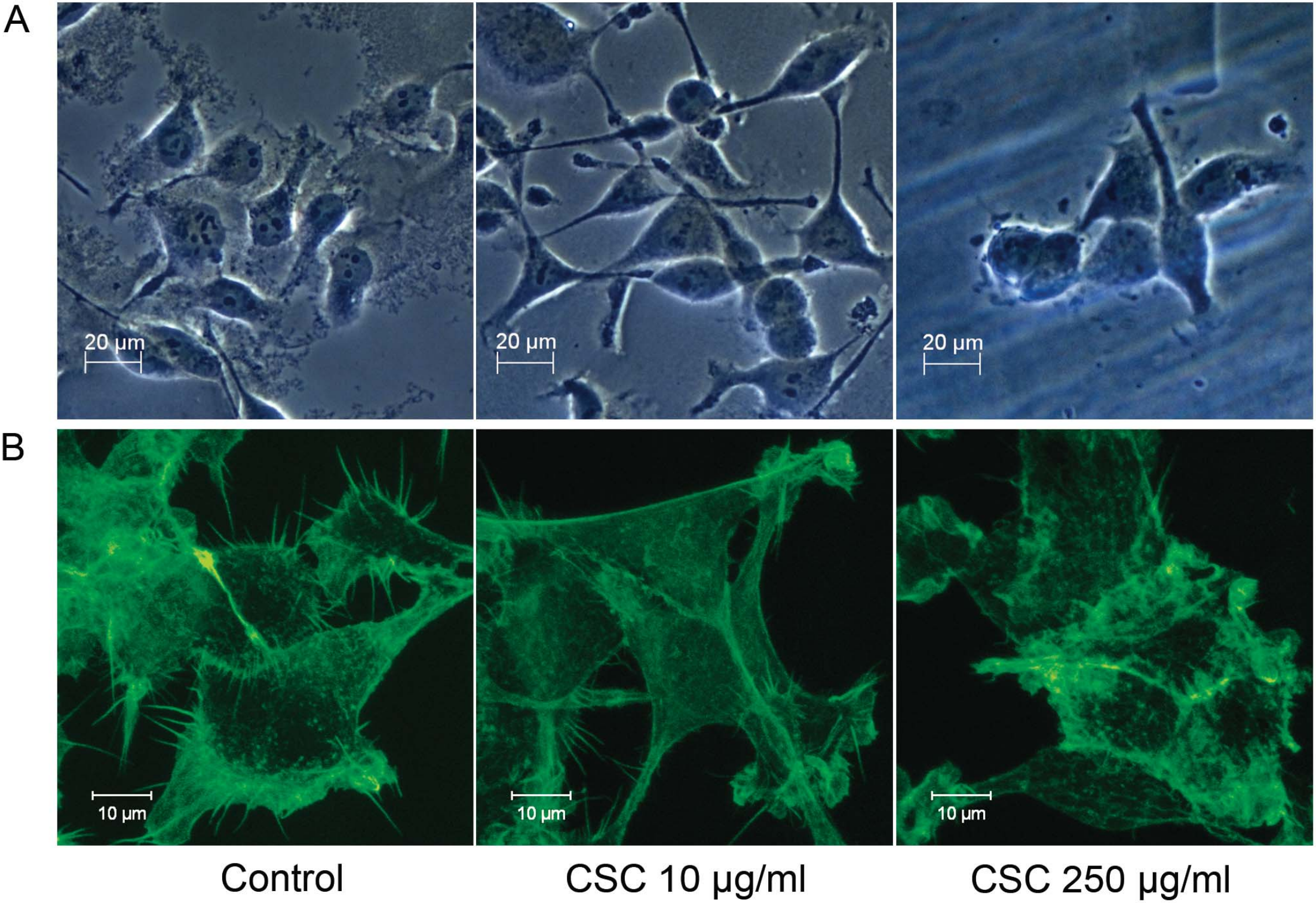
A
20 µm
20 µm
20 µm
B
10 µm
10 µm
10 µm
Control
CSC 10 µg/ml
CSC 250 µg/ml

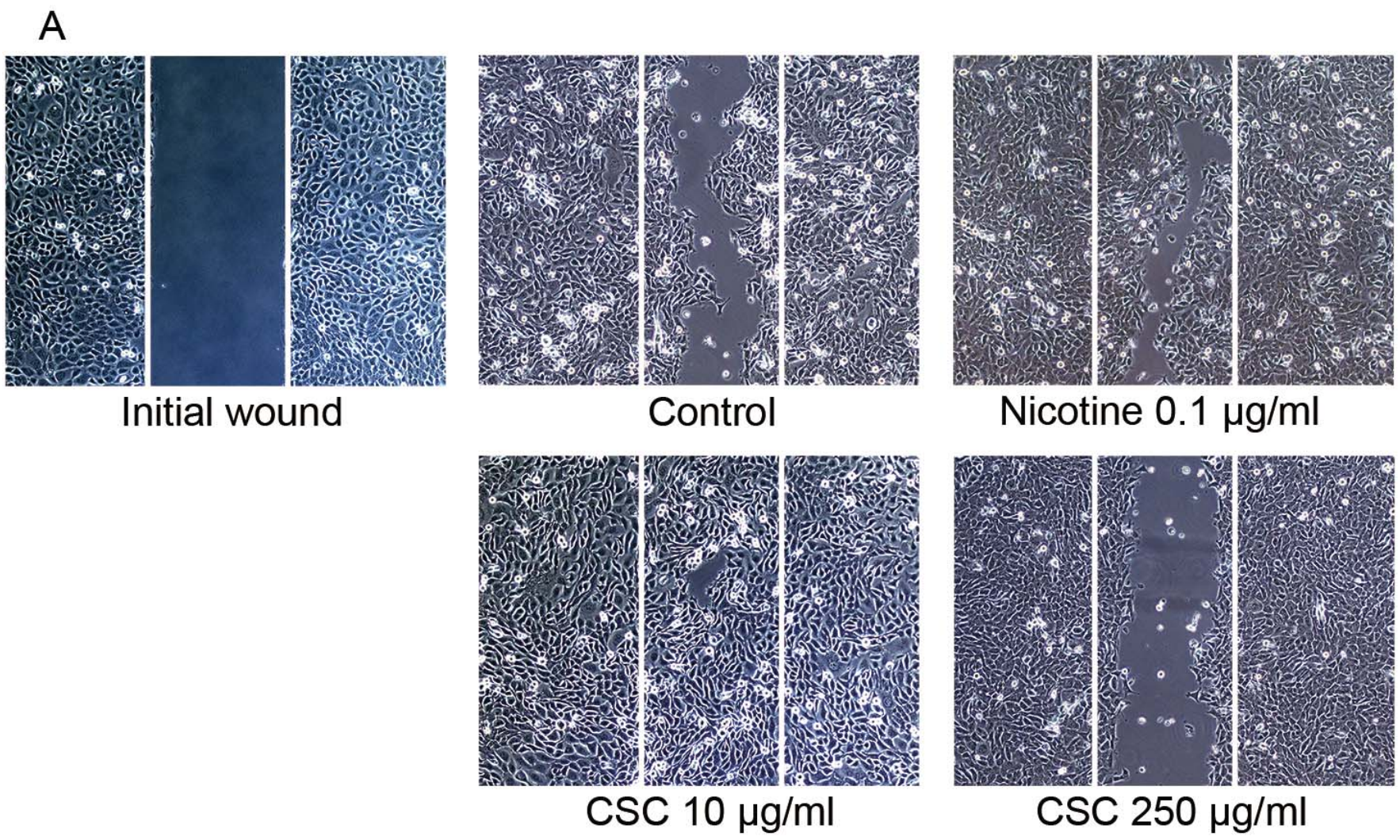
A
Initial wound
Control
Nicotine 0.1 µg/ml
CSC 10 µg/ml
CSC 250 µg/ml

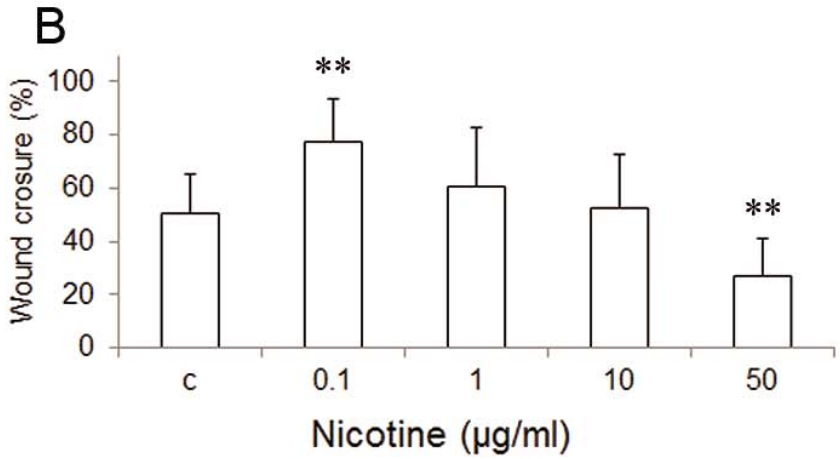
B
Wound crosure (%)
100
80
60
40
20
0
**
**
c
0.1
1
10
50
Nicotine (µg/ml)

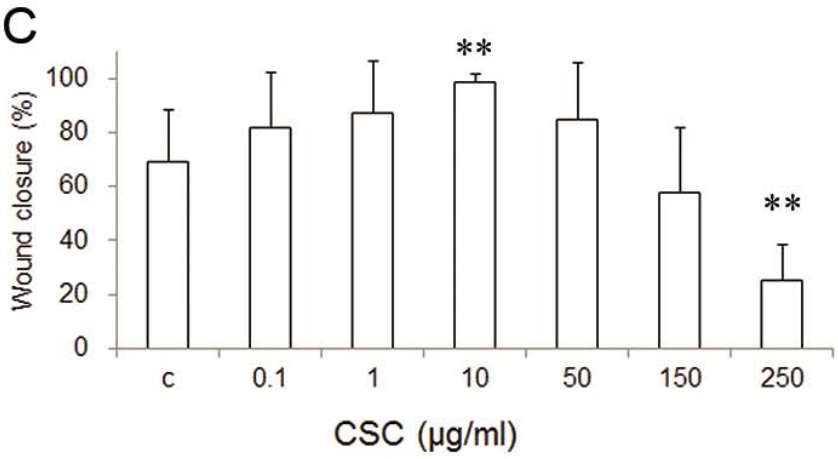
C
Wound closure (%)
100
80
60
40
20
0
**
**
c
0.1
1
10
50
150
250
CSC (µg/ml)

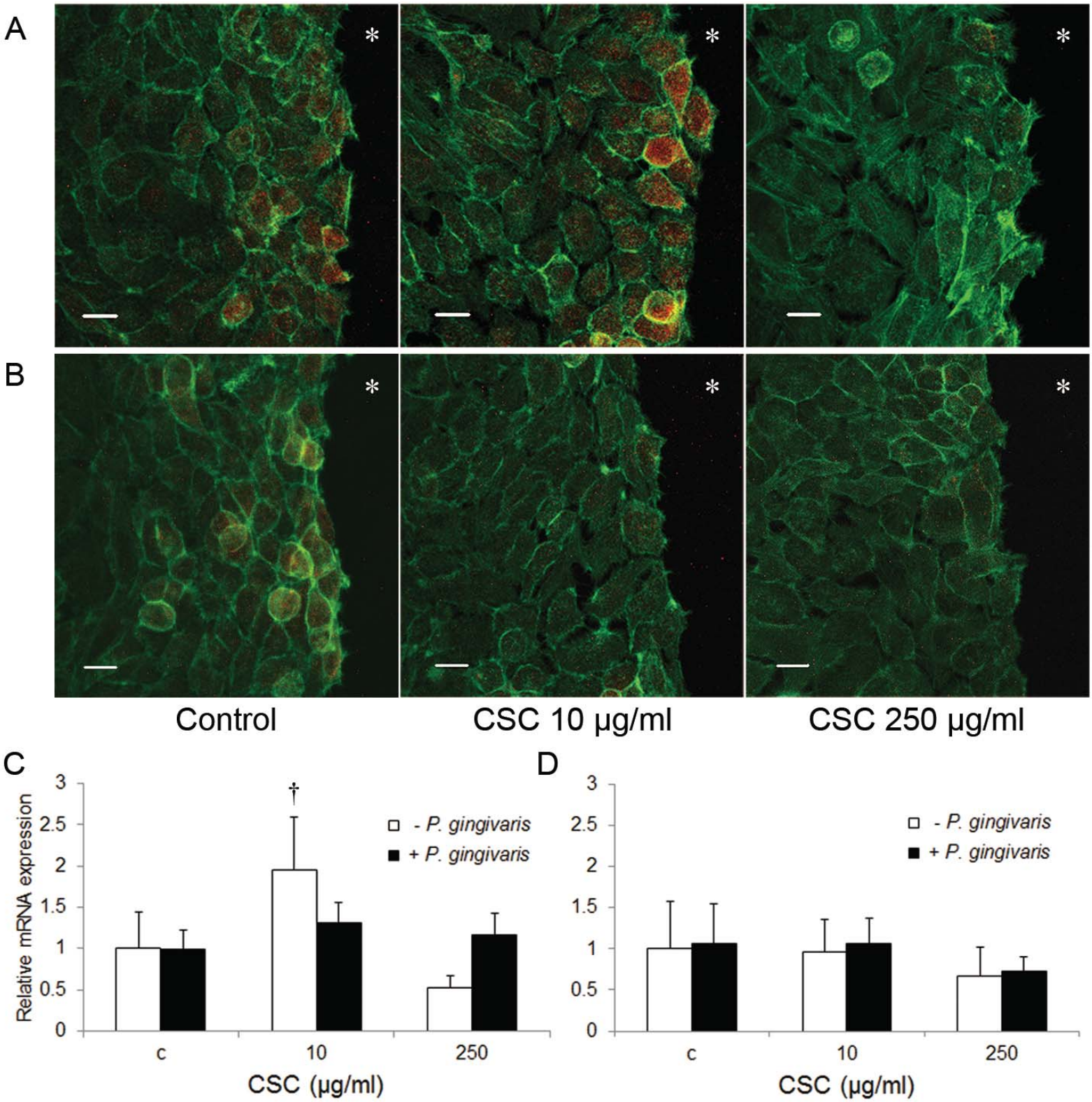
A
B
Control
CSC 10 µg/ml
CSC 250 µg/ml
C
D
Relative mRNA expression
- P. gingivaris
+ P. gingivaris
CSC (µg/ml)
c
10
250
†

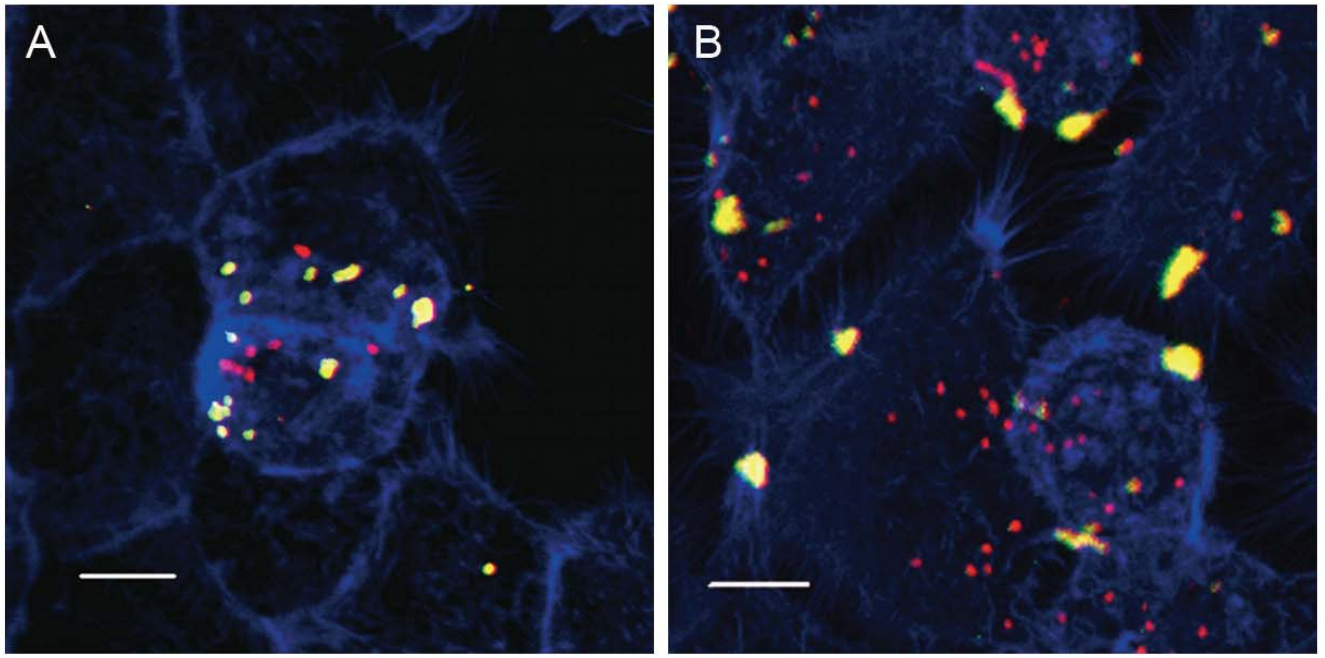
A
B
Control
CSC 1 µg/ml

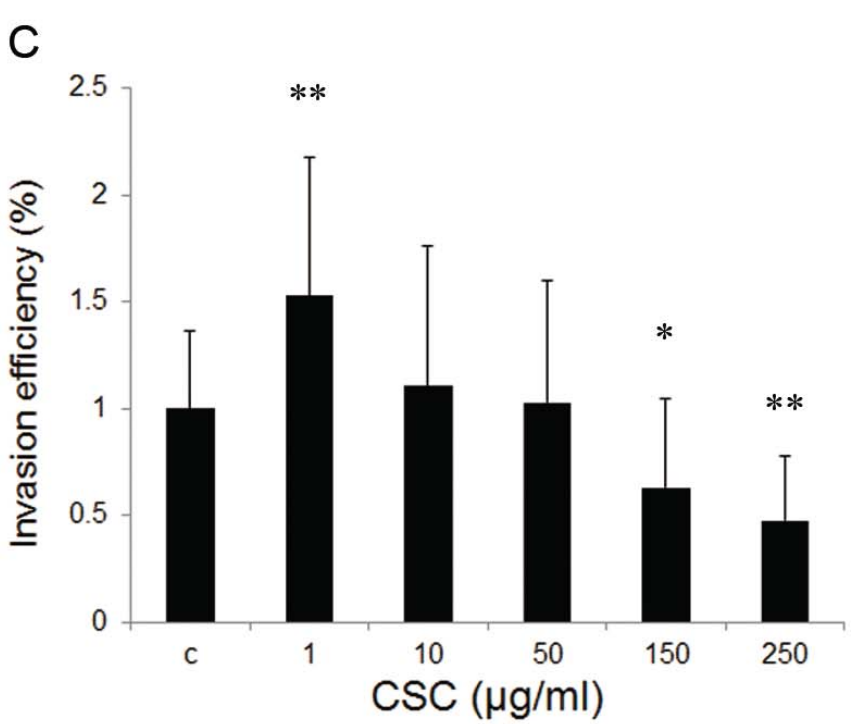
C
Invasion efficiency (%)
2.5
2
1.5
1
0.5
0
**
*
**
c
1
10
50
150
250
CSC (µg/ml)